DOI:
10.1016/j.ydbio.2020.01.006

Document Version
Peer reviewed version

The mTOR pathway component Unkempt regulates neural stem cell and neural progenitor cell cycle in the *Drosophila* central nervous system

Katja T. Maierbrugger[1], Rita Sousa-Nunes[2], Joseph M. Bateman[1#]

[1]Maurice Wohl Clinical Neuroscience Institute

King's College London

125 Coldharbour lane

London

SE5 9NU

UK

[2]Centre for Developmental Neurobiology

King's College London

New Hunts House

Newcomen Street

London SE1 1UL

UK

*Correspondence to: Joseph M. Bateman joseph_matthew.bateman@kcl.ac.uk

Keywords: *Drosophila*; Unkempt; Headcase; mTOR; neurogenesis; neuroblast

Abstract

The formation of a complex nervous system requires the coordinated action of progenitor cell proliferation, differentiation and maturation. The *Drosophila* postembryonic central nervous system provides a powerful model for dissecting the cellular and molecular mechanisms underpinning neurogenesis. We previously identified the conserved zinc finger/RING protein Unkempt (Unk) as a key temporal regulator of neuronal differentiation in the *Drosophila* developing eye and showed that Unk acts downstream of the mechanistic target of rapamycin (mTOR) pathway together with its binding partner Headcase (Hdc). Here we investigate the role of Unk in *Drosophila* postembryonic thoracic neurogenesis. The *Drosophila* central nervous system contains neural stem cells, called neuroblasts, and neural progenitors, known as ganglion mother cells (GMCs). Unk is highly expressed in the central brain and ventral nerve cord but is not required to maintain neuroblast numbers or the regulation of temporal series factor expression in neuroblasts. However, loss of Unk increases the number of neuroblasts and GMCs in S-phase of the cell cycle, resulting in the overproduction of neurons. We also show that Unk interacts with Hdc through its zinc finger domain. The zinc finger domain is required for the synergistic activity of Unk with Hdc during eye development but is not necessary for the activity of Unk in thoracic neurogenesis. Overall, this study shows that Unk and Hdc are novel negative regulators of neurogenesis in *Drosophila* and indicates a conserved role of mTOR signalling in nervous system development.

Introduction

A fundamental challenge during neural development is the correct coordination of cell proliferation and differentiation. This is of particular importance in complex tissues, such as the central nervous system (CNS). During nervous system development, secreted ligands bind specific target receptors on neural stem cells and neural progenitor cells, causing them to exit the cell cycle and undergo a complex program of gene expression and morphological changes resulting in neuronal differentiation (Franco and Muller, 2013; Paridaen and Huttner, 2014; Taverna et al., 2014). Neural development is dependent on progenitor cell proliferation to provide enough cells to generate the mature CNS (Paridaen and Huttner, 2014). This is controlled in a complex spatiotemporal manner and the rate of proliferation and differentiation varies at different stages of development (Franco and Muller, 2013).

Drosophila CNS development and neural stem cell proliferation has proven a powerful model to identify regulatory genes and concepts in neurogenesis (Bello et al., 2008; Truman and Bate, 1988). CNS development in *Drosophila* is characterized by two neurogenic phases, embryonic and postembryonic. The original pool of central brain and ventral nerve cord (VNC) neural stem cells, called neuroblasts in *Drosophila*, is generated early on during embryogenesis by delamination from the neuroepithelium (Doe, 2017). Shortly after, embryonic neuroblasts start dividing asymmetrically to generate neural progenitors called GMCs, that produce the differentiated neurons and glia necessary for larval life. After extensive proliferation in the embryo, neuroblasts undergo a period of quiescence (defined as reversible cell cycle arrest accompanied by low biosynthetic activity), after which proliferation is reactivated in early larval life (Chell and Brand, 2010; Sousa-Nunes et al., 2010; Sousa-Nunes et al., 2011). This second phase of neurogenesis will generate 90 % of neurons that comprise the central brain and VNC of the adult (Harris et al., 2015).

Neuroblast lineages divide asymmetrically in a self-renewable manner. Notch signalling, originally deployed via lateral inhibition to specify neuroblasts, is redeployed along with asymmetric protein complexes to regulate asymmetric neuroblast divisions (Artavanis-Tsakonas and Simpson, 1991; Sousa-Nunes et al., 2010). The vast majority, so-called type I neuroblasts, generate a daughter neuroblast and a single GMC, which divides once to give rise to two post-mitotic neurons/glia (Weng and Lee, 2011). Eight lineages in the central brain, so-called type II neuroblasts, generate a daughter neuroblast and two types of intermediate neural progenitors (INPs), which also divide asymmetrically in turn to produce around 6 GMCs and 12 neurons/glia (Bello et al., 2008; Boone and Doe, 2008; Bowman et al., 2008; Viktorin et al., 2013).

One key feature of neuroblasts and INPs is their ability to generate different types of neuronal progeny over time. This is regulated by a transcriptional cascade called the “temporal series”. The temporal series was first identified in the *Drosophila* embryo and consists of sequential expression of transcription factors (Hb>Svp>Kr>Pdm>Cas) in the neuroblast and its progeny (Brody and Odenwald, 2000; Isshiki et al., 2001; Kambadur et al., 1998). More recently evidence has emerged for a temporal series mechanism in postembryonic lineages (Doe, 2017; Li et al., 2013; Maurange et al., 2008; Suzuki et al., 2013). Type I postembryonic neuroblasts re-entering the cell cycle still express the last transcription factor of the series, Castor (Cas) and subsequently go on to express the orphan nuclear hormone receptor Seven-up (Svp) a second time (Almeida and Bray, 2005; Cenci and Gould, 2005; Maurange et al.,

2008; Shaw et al., 2018). Postembryonic neurons born early express the BTB transcription factor Chinmo, as well as the RNA binding proteins IGF-II mRNA-binding protein (Imp) and Lin-28 (Maurange et al., 2008; Narbonne-Reveau et al., 2016; Zhu et al., 2006), whereas those born late express the BTB transcription factor Broad Complex (Br-C), as well as the RNA binding protein Syncrip (Syp) and Ecdysone-induced protein 93F (Maurange et al., 2008; Syed et al., 2017; Zhu et al., 2006). Cas and Svp, acting upstream of the ecdysone receptor, regulate the early to late born temporal transition, which determines the neuronal identity and eventual post-synaptic targets (Baek and Mann, 2009; Brierley et al., 2012; Maurange et al., 2008; Narbonne-Reveau et al., 2016; Syed et al., 2017).

Regional differences exist in the temporal series mechanisms active in postembryonic neurogenesis. Optic lobe neuroblasts are regulated by a temporal series consisting of Homothorax (Hth)>Klumpfuss (Klu)>Eyeless (Ey)>Sloppy paired 1 and 2 (Slp1 and Slp2)>Dichaete (D)>Tailless (Tll) (Li et al., 2013; Suzuki et al., 2013). Loss-of-function studies have shown that the last four factors are necessary for temporal series progression (Li et al., 2013; Suzuki et al., 2013). Type II neuroblasts express Imp, Lin28, and Chinmo during early larval development and Syp and the Ecdysone receptor B1 (EcRB1) during the late phase (Ren et al., 2017; Syed et al., 2017). Interestingly, INPs are regulated by a distinct temporal series consisting of D>Grh>Ey (Bayraktar and Doe, 2013; Doe, 2017). This temporal series causes early born INPs to produce D or brain-specific homeobox (Bsh) expressing neurons, while late born INPs produce Toy expressing neurons or Repo expressing glia (Bayraktar and Doe, 2013).

Unkempt (Unk) is a zinc finger/RING domain protein expressed in the *Drosophila* nervous system where it plays a role in patterning. Reduced Unk expression results in adult flies with disorganised bristles and rough eyes (Mohler et al., 1992). In the developing eye imaginal disc Unk, along with its binding partner Headcase (Hdc), is required for the correct timing of photoreceptor differentiation (Avet-Rochex et al., 2014). During eye development Unk acts downstream of the insulin receptor/mechanistic target of rapamycin (mTOR) pathway. mTOR signalling downregulates Unk and loss of Unk, or activation of mTOR signalling, causes precocious photoreceptor differentiation (Avet-Rochex et al., 2014). It is not known whether Unk plays a role in neurogenesis in the *Drosophila* CNS.

Here we investigate the requirement for Unk in neurogenesis in the *Drosophila* CNS. We find that Unk is expressed throughout the *Drosophila* CNS and is strongly expressed in

central brain and VNC neuroblasts and their progeny. Unk does not regulate the postembryonic temporal series, nor the number of postembryonic neuroblasts. However, clonal analysis demonstrates that loss of Unk expression increases the number neuroblasts and GMCs in S-phase of the cell cycle, resulting in increased numbers of neurons. Consistent with the role of Unk as a mediator of mTOR signalling, mTOR pathway activity is also required to maintain correct neuronal numbers. Finally, we show that the zinc finger domain of Unk interacts with Hdc but this domain is not necessary for the function of Unk in neurogenesis.

Results

Unk is expressed in neuroblasts, GMCs and neurons in the developing larval CNS

We previously showed that Unk expression is enriched in differentiating photoreceptor neurons, where it is localised to the cytoplasm (Avet-Rochex et al., 2014). To investigate Unk expression in the CNS we first performed western blot analysis on a protein trap line which expresses an Unk::GFP::FLAG fusion protein (Nagarkar-Jaiswal et al., 2015). This shows that in late third instar larvae, Unk::GFP::FLAG expression is much higher in the larval CNS compared to whole larvae (Figure 1A). We next used immunostaining on wild-type and protein trap animals, which shows that in the late third instar, Unk is expressed throughout the CNS but enriched in the central brain and thoracic VNC (Figure 1B, C, Figure 2D-E''). During larval development Unk is strongly expressed in neuroblasts during the first instar and then throughout the neuronal lineage in the second and early third instar larval CNS (Figure 2A-C''). Immunostaining for Miranda, Asense and Prospero were used to visualise neuroblasts, GMCs and neurons respectively (although Prospero is not specific to neurons), and this co-labelling shows that Unk is expressed in the cytoplasm of all three cell types in the late third instar VNC (Figure 1D-F''). Quantification shows that Unk is expressed more strongly in neurons than neuroblasts and GMCs (Supplemental Figure 1A). Thus, Unk expression is enriched throughout the neuronal lineage in the *Drosophila* postembryonic CNS.

Unk does not regulate the temporal series or neuroblast numbers

To investigate a potential role for Unk in postembryonic CNS neurogenesis we focused on thoracic neuroblasts. The temporal series transcription factors Cas and Svp are expressed sequentially and in a non-overlapping manner in neuroblasts, where they determine the identity of neuronal progeny (Maurange et al., 2008). *unk* null mutants survive until the pupal stage, so we first quantified the number of Cas and Svp expressing neuroblasts in *unk* mutant larvae. At 48 hours after larval hatching (ALH) unk^{ex24}/unk^{Df59} null heteroallelic larvae have similar numbers of Cas and Svp expressing Deadpan (Dpn) co-expressing VNC neuroblasts as controls (Figure 3A-F). Thus, Unk does not regulate Cas or Svp expression or neuroblast numbers at this stage. To confirm that Unk does not alter neuroblast numbers, Dpn expressing thoracic neuroblasts were quantified in late third instar larvae (96 hours ALH). unk^{ex24}/unk^{Df59} larvae have similar numbers of thoracic neuroblasts as controls (Figure 3G-I). Moreover, late third instar unk^{ex24} mutant neuronal thoracic mosaic analysis with a repressible cell marker (MARCM; (Lee and Luo, 1999)) clones always have a single neuroblast (Figure 3J-K''). *unk* null mutants are lethal during mid-pupal development (Avet-Rochex et al., 2014; Mohler et al., 1992), but unk^{ex24}/unk^{Df59} null mutants still have similar numbers of thoracic neuroblasts as controls at ten hours after pupal formation (APF; Supplemental Figure S1B-D). Therefore, loss of Unk expression does not affect the temporal series or neuroblast numbers during larval development.

Loss of Unk increases EdU incorporation in neuroblasts and GMCs

Type I neuroblasts divide asymmetrically to generate a daughter neuroblast and a GMC. GMCs are neural progenitors that then divide symmetrically to generate two neurons/glia. To determine whether loss of Unk affects GMCs we quantified Asense, which is expressed exclusively in neuroblasts and GMCs in type I lineages. Consistent with the lack of an effect on neuroblasts, *unk* mutant clones have similar numbers of Asense expressing cells as controls (Figure 4A-C). To analyse whether Unk regulates the cell cycle in neuroblasts and GMCs we used 5-ethynyl-2'-deoxyuridine (EdU) labelling. Interestingly, *unk* mutant clones have significantly more EdU labelled cells than controls at both 48 hours and 72 hours ALH (Figure 4D-G). Moreover, the proportion of neuroblasts incorporating EdU is significantly increased in *unk* mutant clones at 48 hours ALH, but similar to controls at 72 hours ALH (Figure 4H, I). The fact that the number of EdU-positive cells per clone is more than the number of GMCs per clone, indicates that EdU is being inherited by GMC progeny and that

this is occurring faster in *unk* mutant clones than in controls. Altogether, we conclude that Unk is necessary to maintain normal S-phase in neuroblasts and GMCs.

Unk, Hdc and mTOR signalling regulate neurogenesis

We surmised that if Unk is required to maintain S-phase in neuroblasts and GMCs then *unk* mutant clones should contain more neurons. In accordance with this prediction, quantification of cell number using nuclear-RFP expression shows that late third instar *unk* mutant neuronal thoracic VNC MARCM clones contain significantly more cells than controls (Figure 5A, B, F). Unk and Hdc are components of the mTOR pathway, negatively regulated by mTOR, and required for timely photoreceptor differentiation in *Drosophila* (Avet-Rochex et al., 2014). Hdc is expressed in a similar pattern to Unk in the larval CNS and is also cytoplasmically localised (Supplemental Figure S1E-G''). Similar to *unk* clones, *hdc* mutant clones contain significantly more cells than controls (Figure 5A, C, F). In agreement with a previous study (Cheng et al., 2011), we found that thoracic VNC clones mutant for the mTOR pathway negative regulator *Tsc1* contain significantly more cells than controls (Figure 5A, D, F), similar to clones mutant for *unk* and *hdc* (Figure 5A-C, F). Conversely, and in accordance with its role as a positive regulator of the mTOR pathway, although in contrast to a previous study (Cheng et al., 2011), clones mutant for *Rheb* contain significantly fewer cells than controls (Figure 5E, F). Loss of *unk* suppresses the *Rheb* mutant phenotype, as clones mutant for both *unk* and *Rheb* have similar numbers of cells to controls (Figure 5F), consistent with Unk acting downstream of mTOR (Avet-Rochex et al., 2014; Li et al., 2019). We conclude that Unk, Hdc and the mTOR pathway regulate the cell cycle in neural stem cells and neural progenitors in the postembryonic thoracic VNC, with Unk and Hdc acting as negative regulators.

Unk physically interacts with Hdc via its zinc finger domain

Unk contains highly conserved zinc finger and RING domains (Figure 6A) and genetically and physically interacts with Hdc to regulate neurogenesis (Avet-Rochex et al., 2014; Li et al., 2019), but the structural basis of this interaction is not known. In mammals, structure function analysis revealed that Unk regulates cortical neural progenitor morphology and migration through binding of the zinc finger domain to mRNAs, which regulates mRNA

translation (Murn et al., 2016; Murn et al., 2015). In order to begin to understand how the interaction between Unk and Hdc might regulate neurogenesis in *Drosophila*, we investigated how they physically interact. We generated HA-tagged full-length and deletion mutants in Unk that lack either the N-terminal zinc finger domain (HA-UnkΔZF), the unstructured middle region (HA-UnkΔMid), or the C-terminal RING domain (HA-UnkΔRING) (Figure 5A). Expression of these constructs in S2 cells confirms that the proteins have the expected molecular weights (Supplemental Figure S2A). Co-expression of these deletion mutants with FLAG-Hdc in S2 cells and immunoprecipitation of Hdc using an anti-FLAG antibody shows that full-length HA-Unk, HA-UnkΔMid and HA-UnkΔRING co-immunoprecipitate with Hdc, whereas HA-UnkΔZF does not (Figure 6B). Therefore, the zinc finger domain is required for Unk to physically interact with Hdc. We also find that the C-terminal half of Unk containing the zinc finger domain (HA-UnkZF-FL, Supplemental Figure S2B) is sufficient to interact with Hdc (Figure 6C, D). Moreover, using constructs containing all six zinc fingers (HA-UnkZF1-6), zinc fingers 1-3 (HA-UnkZF1-3), or 4-6 (HA-UnkZF4-6), (Supplemental Figure 2C, D), we find that Unk zinc fingers 1-3 are necessary and sufficient to physically interact Hdc (Figure 6C, D). Therefore, Unk and Hdc physically interact via the first half of the zinc finger domains in Unk.

The zinc finger domain in Unk is required for its synergistic activity with Hdc during eye development

We next used an overexpression assay to determine which domain of Unk is necessary for its function and interaction with Hdc *in vivo* during eye development. Simultaneous overexpression of Unk and Hdc in the developing eye delays photoreceptor differentiation and causes a rough eye phenotype in the adult, while overexpression of Unk or Hdc alone have no effect (Avet-Rochex et al., 2014). We generated flies expressing HA-tagged full-length Unk or Unk deletion mutants (Figure 7A) and confirmed that these proteins have the expected molecular weights when overexpressed in the CNS (Supplemental Figure S3) and that HA-tagged Unk produces a rough eye phenotype when overexpressed with Hdc (Figure 7E). We then tested the Unk deletion mutants for their ability to cause a rough eye phenotype when overexpressed together with Hdc in the eye using *GMR-GAL4*. Similar to full-length Unk, none of the Unk mutant forms cause an eye phenotype when overexpressed alone with *GMR-GAL4* (Figure 7F-H). When overexpressed with Hdc however, Unk lacking the middle

region (UnkΔMid-HA) or the RING domain (UnkΔRING-HA) produce a rough eye, whereas Unk lacking the zinc finger domain (UnkΔZF-HA) does not produce a rough eye phenotype (Figure 7I-K). Consistent with the Unk-Hdc co-immunoprecipitation results (Figure 6B), these data suggest that the middle region and RING domain are not required for Unk to interact with Hdc. Loss of the zinc finger domain prevents Unk from interacting with Hdc and so UnkΔZF-HA is not functional in this co-overexpression assay (Figure 7I). However, the zinc finger domain could be required for Unk to function alone, regardless of its interaction with Hdc, and this may also be why UnkΔZF-HA does not cause a synergistic rough eye phenotype with Hdc.

The zinc finger domain of Unk is not required to regulate neurogenesis

The structure-function analysis of Unk described above shows that the zinc finger domain is necessary to perturb photoreceptor development when overexpressed together with Hdc. To dissect the structure-functional requirements of Unk during neurogenesis in the CNS we performed rescue experiments by expressing the different Unk deletion mutants in unk^{ex24} mutant MARCM clones in the postembryonic thoracic VNC. Over-expression of full length Unk and the deletion mutants using *Elav-Gal4* shows that they are all robustly expressed in the larval CNS and that overexpression does not alter neuronal numbers in the VNC (Supplemental Figure S4). Surprisingly, Unk mutants lacking the zinc finger, middle region or RING domain all rescue the increase in neuronal cell number caused by loss of Unk expression in unk^{ex24} clones (Figure 8A). These data show that no single domain of Unk is absolutely required for its role in the regulation of neurogenesis.

Discussion

Unk is a highly conserved zinc finger/RING domain protein and a component of the mTOR pathway but its role in *Drosophila* CNS development has not been investigated. We have shown that Unk and its binding partner Hdc are strongly expressed in the postembryonic CNS. Although Unk is expressed in neuroblasts, loss of Unk does not affect the temporal series that determines the identity of differentiating neurons. Rather, loss of Unk alters the cell cycle in neuroblasts and GMCs resulting in increased neurogenesis, consistent with its role as a negative regulator of mTOR signalling (Figure 8B). Finally, structure function

analysis shows that the zinc finger domain of Unk is required for its interaction with Hdc but is not required for its role in the regulation of neurogenesis. We conclude that Unk is a novel regulator of neurogenesis in the *Drosophila* CNS.

Temporal regulators of neuronal identity are defined by their requirement to establish specific neuronal fates. For example, in type I neuroblasts the orphan nuclear hormone receptor Svp is absolutely required for the switch from early to late born neuronal fates (Maurange et al., 2008). Svp is similarly required in type II neuroblasts, where is regulates ecdysone receptor (EcR) expression and loss of the EcR also prevents the switch from early to late born fates (Syed et al., 2017). In the developing eye imaginal disc loss of Unk does not alter photoreceptor identity but causes precocious differentiation of photoreceptor neurons, resulting in patterning defects in the adult eye (Avet-Rochex et al., 2014; Bateman and McNeill, 2004; McNeill et al., 2008). Similarly, in the postembryonic CNS Unk is not required for neurons to acquire their identity, but regulates the numbers of neurons generated through control of the cell cycle in neuroblasts and GMCs. Loss of Unk expression causes increased EdU incorporation in neuroblasts and GMCs during early (48 hours ALH) larval development, suggesting that Unk has a particularly important role at this stage. Mis-regulation of the cell cycle is not sufficient to increase the number of neuroblasts or GMCs, but results in an increase in the number of post-mitotic neurons by the end of larval development. The precise mechanism by which this increase occurs requires further investigation, and we cannot exclude the possibility the loss of Unk causes GMCs to divide more than once. Early and late born postembryonic thoracic motor neurons innervate specific domains of adult leg muscles (Baek and Mann, 2009; Brierley et al., 2012). Loss of Unk and the resulting deregulation of neurogenesis may therefore affect motor circuits controlling locomotion.

mTOR signalling plays key roles in mammalian neurogenesis (Bateman, 2015; Bateman and McNeill, 2006; Tee et al., 2016). *In utero* electroporation experiments using overexpression of a constitutively active form of Rheb have revealed the requirements for mTOR signalling in the mammalian subventricular zone. Activation of mTOR signalling caused precocious differentiation of highly proliferative Mash1-expressing transit amplifying cells, at the expense of self-renewal, resulting in increased numbers of neurons (Hartman et al., 2013). We previously showed that loss of Unk or activation of mTOR signalling causes precocious differentiation of photoreceptor neurons (Avet-Rochex et al., 2014). In the current study we have shown that clones mutant for *unk* have more EdU-incorporation in neuroblasts and

GMCs and increased numbers of neurons. Together these studies point to a conserved role for Unk and mTOR signalling in regulating the cell cycle in neural stem cells and neural progenitors and their differentiation into neurons (Figure 8B).

Although Unk acts downstream of the mTOR pathway, unlike other mTOR pathway components Unk does not regulate cell growth in nutrient rich conditions (Avet-Rochex et al., 2014; Bateman, 2015; Li et al., 2019; Tee et al., 2016). However, a recent study showed that Unk and Hdc negatively regulate tissue growth under nutrient restriction in *Drosophila* (Li et al., 2019). Clones mutant for *unk* or *hdc* in the eye or wing imaginal disc are larger than controls and have accelerated cell cycle progression only in larvae fed a low protein diet. The ability of Unk and Hdc to regulate mitotic cell proliferation under nutrient restriction requires mTOR pathway activity, consistent with the role of these proteins as mTOR pathway components. The precise role of Unk in the mTOR pathway remains to be determined. Although, Li *et al*., (2019) found that Unk physically interacts with the mTOR complex 1 (mTORC1) component Raptor. Moreover, a mass spectrometry analysis of the insulin receptor/mTOR proteome in *Drosophila* showed that Unk physically interacts with Raptor, mTOR and 4E-BP (Glatter et al., 2011). Therefore, Unk may be a component of mTORC1.

Physical interaction of Unk and Hdc in *Drosophila* has been observed in multiple independent studies (Avet-Rochex et al., 2014; Giot et al., 2003; Glatter et al., 2011; Li et al., 2019; Veraksa et al., 2005). In the current study, we define the first half of the zinc finger domain in Unk as necessary and sufficient for the interaction with Hdc. In keeping with our co-immunoprecipitation experiments, using a yeast-2-hydrid screen Li et al., (2019) found that amino acids 94-154 in Unk, which includes part of the second and all the third zinc finger (Supplemental Figure S5), are necessary for the physical interaction with Hdc. Mammalian UNK also physically interacts with the Hdc ortholog HECA (Li et al., 2019) and so the interaction of these binding partners is evolutionarily conserved.

Unk is a highly conserved protein and recent studies have provided insight into the function of UNK in mammals. The zinc finger domain of mammalian UNK was shown to bind mRNAs and to negatively regulate the translation of these targets in neuroblastoma cells (Murn et al., 2016; Murn et al., 2015). UNK binds the transcripts of several hundred genes with diverse functions, including regulators of translation and S6K signalling. We found that the zinc finger domain of *Drosophila* Unk is not required to rescue the increase in number of

neurons in *unk* mutant MARCM clones. The role of the zinc finger domain may therefore vary depending on the context or cell type.

UNK is strongly expressed in the murine brain and knock-down of UNK in the developing cortex causes defects in the migration and morphology of neural progenitors (Murn et al., 2015). Although these phenotypes need to be confirmed using knock-out approaches, they suggest the exciting possibility that Unk plays a conserved role in nervous system development. Further characterisation of Unk using invertebrate and vertebrate models will decipher the role(s) of this highly conserved protein in the nervous system.

Materials and Methods

Fly strains and growth conditions

Flies were maintained on standard food (per litre: 6.4 g Agar (Fisher), 64 g glucose (Sigma), 16 g ground yellow corn and 80 g Brewer's yeast (MP Biomed Europe), 3 ml propionic acid (Fisher), 1.8 g methyl 4-hydroxybenzoate (Sigma), 16 ml ethanol (Sigma)) at 25^{o}C in a 12 hour light/dark cycle unless stated otherwise. Genotypes for all experiments are described in Supplemental Table S1. Fly stocks were *elav-GAL4^{C155}, UAS-Redstinger, hsFLP^{122}; FRT82B, tub-GAL80* (a gift from Darren Williams), *FRT82B,unk^{ex24}* (Avet-Rochex et al., 2014), *FRT82B,unk^{Df59}* (Avet-Rochex et al., 2014), *UAS-hdcFL* (Steneberg and Samakovlis, 2001), *FRT82B,Tsc1^{Q600X}* (Potter et al., 2001), *FRT82B,Rheb^{2D1}* (Stocker et al., 2003), *FRT82B,hdc^{43}* (Weaver and White, 1995). Fly stocks from the Bloomington Drosophila stock Center were *Da-GAL4, hs-GAL4, tub-GAL80^{ts}, GMR-GAL4, Unk::GFP::FLAG* (*Mi{PT-GFSTF.2}unk$^{MI09783\text{-}GFSTF.2}$*).

MARCM mutant clones were generated via a heat shock for 1.5 hours at 37°C 24 hours after a 4-hour egg lay. Larvae were collected for dissection once leaving the food (wandering) at the third instar larval stage. For dissections at earlier time points, larvae were staged at the first instar. First instar larvae were kept at 25°C for 48 hours or 72 hours and larvae isolated by floating following submerging the food in 30 % (v/v) glycerol in PBS (Thermo Fisher).

Western blot analysis

For *Hs-GAL4* induced transgene expression, wandering late third instar larvae were heat-shocked for 90 minutes at 37°C, then transferred to 29°C for 3 hours. Whole larvae or larval CNS tissue were collected and first washed in PBS. 150 µl per 20 larvae and 50 µl per 10 CNSs of 1x SDS buffer (62.5 mM Tris HCl pH 6.8, 2 % (w/v) SDS (Sodium Dodecyl Sulphate, VWR International), 10 % glycerol (Sigma-Aldrich) and 0.01 % (w/v) bromophenol blue) and 10 % (v/v) 1 M Dithiothreitol (DTT, Thermo Fisher Scientific) were added to each tube and the tissue homogenised using sterile pestles. The proteins were denatured at 98°C for 5 minutes and after centrifuged at 1200 x g. The supernatant was removed, and the centrifugation step repeated. The extracted protein was stored at -20°C. Primary antibodies were mouse anti-GFP (Invitrogen 3E6, 1/1000), mouse anti-HA (New England Biolabs 6E2, 1/1000), mouse anti-FLAG (M2 Agilent 200472, 1/1000), rabbit anti-Actin (Cell Signalling 4967S, 1/5000). Secondary antibodies were anti-mouse Alexa Fluor 680 (Invitrogen A21058), anti-rabbit IR Dye 800 (LICOR 926-32211).

5-ethynyl-2'-deoxyuridine (EdU) incorporation and immunofluorescence

CNS tissue was fixed for 30 minutes on ice in 4 % (v/v) formaldehyde (Thermo Fisher) in PBS, then immunostained as in (Avet-Rochex et al., 2014) and (Avet-Rochex et al., 2012). For EdU staining the Click-iT EdU Imaging Kit (Thermo Fisher Scientific) was utilised. A 10 mM EdU stock solution was diluted 1/1000 in Schneider's medium (Invitrogen) and 500 µl prepared into microcentrifuge tubes. Six CNSs per condition were dissected in PBS then transferred into the EdU-Schneider's solution. CNS were incubated for 2 hours at 25°C. After EdU removal, the tissue was fixed in 4 % paraformaldehyde for 30 minutes. The fixative was removed and the tissue washed five times for 10 minutes with PBS 0.1% Triton-X100 (Sigma, PBS-T). Meanwhile fresh Click-iT reaction cocktail was prepared according to manufacturer's instructions. After the final wash the Click-iT reaction cocktail was added and CNSs and incubated for 30 minutes protected from light. Then the cocktail was removed, CNSs were washed five times for 10 minutes with PBS-T, mounted in Vectashield on glass slides and stored at 4°C in the dark. Primary antibodies were rat anti-Unk3 (Avet-Rochex et al., 2014), 1/500), mouse anti-Hdc (a gift from Robert White, 1/5), rat anti-Chinmo (a gift from Nikolas Sokol, 1/500), rabbit anti-Cas (a gift from Stefan Thor, 1/250), mouse anti-Svp (DSHB, 1/250), Guinea pig anti-Deadpan (a gift from Jürgen Knoblich, 1/1000), rat anti-Asense (a gift from Jürgen Knoblich, 1/1000), rabbit anti-Miranda (a gift from Frank Hirth,

1/200), mouse anti-Prospero (DSHB, 1/10). Secondary antibodies were all used at 1/1000 and were anti-mouse Alexa Fluor 488 (Thermo Fisher Scientific A11001), anti-mouse Alexa Fluor 546 (Life Tech A11030), anti-mouse Alexa Fluor 633 (Thermo Fisher Scientific A21050), anti-rat Alexa Fluor 488 (Thermo Fisher Scientific A11006), anti-rat Alexa Fluor 555 (Thermo Fisher Scientific A214340), anti-rabbit Alexa Fluor 488 (Thermo Fisher Scientific A11034), anti-rabbit Alexa Fluor 546 (Thermo Fisher Scientific A11010), anti-guinea pig Alexa Fluor 555 (Thermo Fisher Scientific A21435).

Microscopy and image quantification

All images were acquired using a Zeiss LSM710 or a Nikon A1R confocal microscope. Neuroblasts were quantified manually by counting all Dpn or Miranda positive cells in the VNC or by counting all cells positive for Dpn and Svp or Cas. Asense-positive cells and EdU positive cells were quantified manually. The proportion of EdU positive neuroblasts was determined by counting the number of EdU positive neuroblasts in MARCM clones as a proportion of the total number of MARCM clones in each VNC. Nuclear-RFP expressing cells in MARCM clones were quantified using the measurement tool in Volocity (Version 6.3, PerkinElmer Inc.).

Generation of Unk constructs

Unk constructs were generated by PCR from pENTR-unk (Avet-Rochex et al., 2014) using the primers in Supplemental Table S2 and cloned into pENTR/D-TOPO. To generate the UnkΔMid constructs a two-stage method was used. First two overlapping PCR products were generated using primers UnkFWEntr with UnkΔMid.Rv and UnkΔMid.Fw with UnkRVfusionEntr (Supplemental Table S2). These overlapping PCR products were then used together with primers UnkFWEntr and UnkRVfusionEntr to generate an Unk cDNA lacking the middle region, which was cloned into pENTR/D-TOPO. All constructs were confirmed by Sanger sequencing. For tissue culture expression, Unk constructs were recombined into the pAHW (DGRC) destination vector to generate N-terminal HA-tagged fusions. For transgenic expression Unk constructs were recombined into the pUASg-HA.attB (Bischof et al., 2013) destination vector to generate C-terminal HA-tagged fusions. Recombination into destinations vectors was performed using the Gateway LR Clonase II kit (ThermoFisher)

according to the manufacturer's instructions. Transgenic constructs were targeted to the attP2 landing site (68A4, BDSC#8622) via phiC31 integrase-mediated transgenesis.

Co-immunoprecipitation

Drosophila S2 Schneider cells were maintained in Sf-900 III SFM insect cell culture medium (Gibco Thermo Fisher Scientific) containing 10 % (v/v) heat-inactivated fetal-bovine-serum (FBS, Sigma-Aldrich), 50 U/ml penicillin and 50 µg/ml streptomycin (Thermo Fisher Scientific) at 25°C. For transfection, cells were seeded at a density of approximately 2.5 million cells per well in a 6-well plate (Thermo Fisher Scientific) in S2 cell media without antibiotics. Dm160 (a gift from Nic Tapon) encoding GFP in pAFW (DGRC) was used to express FLAG-GFP as a negative control. Two wells per condition were transfected the next day using Fugene transfection reagent (Promega E2311). Unk constructs were co-transfected with FLAG-tagged Hdc (Avet-Rochex et al., 2014). For co-immunoprecipitation assays cells were lysed in 500 µl lysis buffer containing: 25 mM Tris pH 8, 150 mM NaCl, 1 % triton X-100, 5 % glycerol and freshly added 1x protease inhibitor cocktail (Roche) and 1mM PMSF (Sigma-Aldrich). Cells were lysed by pipetting up and down and incubated on a rotator at 40 rpm at 4°C for 1 hour. The lysates were then pelleted at 15300 x g at 4°C for 10 minutes to remove cell debris and the remaining lysate was transferred into fresh microcentrifuge tubes. 4 µg of rabbit anti-FLAG (Sigma F7425-.2MG) was added to each condition and incubated on a rotator at 10 rpm at 4°C overnight. 20 µl (10 µl bead volume) of protein G beads (Fisher 10229283) per condition were washed twice in ice-cold sterile PBS and then resuspended in 500 µl of ice-cold lysis buffer. The lysates were incubated with the beads at 10 rpm for 4 hours at 4°C. The beads were pelleted at 2650 x g at 4°C for 30 seconds, the supernatant was removed, and the beads were washed once in 500 µl ice-cold lysis buffer and twice in 500 µl ice-cold wash buffer containing: 25 mM Tris pH 8, 150 mM NaCl. The bound protein was released by adding 30 µl 2x SDS-buffer containing: 125 mM Tris HCl pH 6.8, 4 % (w/v) SDS, 20 % glycerol and 0.02 % (w/v) bromophenol blue. The proteins were denatured at 96°C for 10 minutes, the beads were pelleted at 15300 x g for 1 minute at room temperature, after which the supernatant containing the co-immunoprecipitated proteins were analysed by western blot. Primary antibodies were mouse anti-HA (6E2 New England Biolabs, 1/1000), mouse anti-FLAG (M2 Agilent 200472, 1/1000), rabbit anti-FLAG (Sigma F7425-.2MG, for immunoprecipitation, 4µg per condition), rabbit anti-Actin (Cell Signalling

4967S, 1/5000). Secondary antibodies were anti-mouse Alexa Fluor 680 (Invitrogen A21058), anti-rabbit IR Dye 800 (LICOR 926-32211).

Statistical analysis

Comparison of two sets of continuous data were analysed using the two-tailed, unpaired student's t-test. Equal variance was analysed using the F-test. If samples were of unequal variance, the Welch's correction was applied to the student's t-test. To compare data of more than two sets one-way analysis of variance (ANOVA) was used followed by Dunnett's or Tukey's post-hoc tests. GraphPad Prism (Version 7, GraphPad Software Inc.) was used for statistical analysis and to generate graphs.

Acknowledgements

We thank Darren Williams for fly stocks, Robert White, Stefan Thor, Nikolas Sokol, Jürgen Knoblich and Frank Hirth for antibodies and Nic Tapon for the DM160 plasmid. Fly stocks were obtained from the Bloomington Drosophila Stock Center (NIH P40OD018537) were used in this study. We thank the Wohl Cellular Imaging Centre at King's College London for help with light microscopy. This work was funded by a King's College London Graduate Teaching Award.

References

Almeida, M.S., Bray, S.J., 2005. Regulation of post-embryonic neuroblasts by Drosophila Grainyhead. Mech Dev 122, 1282-1293.

Artavanis-Tsakonas, S., Simpson, P., 1991. Choosing a cell fate: a view from the Notch locus. Trends Genet 7, 403-408.

Avet-Rochex, A., Carvajal, N., Christoforou, C.P., Yeung, K., Maierbrugger, K.T., Hobbs, C., Lalli, G., Cagin, U., Plachot, C., McNeill, H., Bateman, J.M., 2014. Unkempt is negatively regulated by mTOR and uncouples neuronal differentiation from growth control. PLoS Genet 10, e1004624.

Avet-Rochex, A., Kaul, A.K., Gatt, A.P., McNeill, H., Bateman, J.M., 2012. Concerted control of gliogenesis by InR/TOR and FGF signalling in the Drosophila post-embryonic brain. Development 139, 2763-2772.
Baek, M., Mann, R.S., 2009. Lineage and birth date specify motor neuron targeting and dendritic architecture in adult Drosophila. J Neurosci 29, 6904-6916.
Bateman, J.M., 2015. Mechanistic insights into the role of mTOR signaling in neuronal differentiation. Neurogenesis (Austin, Tex.) 2, e1058684.
Bateman, J.M., McNeill, H., 2004. Temporal control of differentiation by the insulin receptor/tor pathway in Drosophila. Cell 119, 87-96.
Bateman, J.M., McNeill, H., 2006. Insulin/IGF signalling in neurogenesis. Cell Mol Life Sci 63, 1701-1705.
Bayraktar, O.A., Doe, C.Q., 2013. Combinatorial temporal patterning in progenitors expands neural diversity. Nature 498, 449-455.
Bello, B.C., Izergina, N., Caussinus, E., Reichert, H., 2008. Amplification of neural stem cell proliferation by intermediate progenitor cells in Drosophila brain development. Neural development 3, 5.
Bischof, J., Bjorklund, M., Furger, E., Schertel, C., Taipale, J., Basler, K., 2013. A versatile platform for creating a comprehensive UAS-ORFeome library in Drosophila. Development 140, 2434-2442.
Boone, J.Q., Doe, C.Q., 2008. Identification of Drosophila type II neuroblast lineages containing transit amplifying ganglion mother cells. Developmental neurobiology 68, 1185-1195.
Bowman, S.K., Rolland, V., Betschinger, J., Kinsey, K.A., Emery, G., Knoblich, J.A., 2008. The tumor suppressors Brat and Numb regulate transit-amplifying neuroblast lineages in Drosophila. Dev Cell 14, 535-546.
Brierley, D.J., Rathore, K., VijayRaghavan, K., Williams, D.W., 2012. Developmental origins and architecture of Drosophila leg motoneurons. The Journal of comparative neurology 520, 1629-1649.
Brody, T., Odenwald, W.F., 2000. Programmed transformations in neuroblast gene expression during Drosophila CNS lineage development. Dev Biol 226, 34-44.
Cenci, C., Gould, A.P., 2005. Drosophila Grainyhead specifies late programmes of neural proliferation by regulating the mitotic activity and Hox-dependent apoptosis of neuroblasts. Development 132, 3835-3845.

Chell, J.M., Brand, A.H., 2010. Nutrition-responsive glia control exit of neural stem cells from quiescence. Cell 143, 1161-1173.
Cheng, L.Y., Bailey, A.P., Leevers, S.J., Ragan, T.J., Driscoll, P.C., Gould, A.P., 2011. Anaplastic lymphoma kinase spares organ growth during nutrient restriction in Drosophila. Cell 146, 435-447.
Doe, C.Q., 2017. Temporal Patterning in the Drosophila CNS. Annu Rev Cell Dev Biol 33, 219-240.
Franco, S.J., Muller, U., 2013. Shaping our minds: stem and progenitor cell diversity in the mammalian neocortex. Neuron 77, 19-34.
Giot, L., Bader, J.S., Brouwer, C., Chaudhuri, A., Kuang, B., Li, Y., Hao, Y.L., Ooi, C.E., Godwin, B., Vitols, E., Vijayadamodar, G., Pochart, P., Machineni, H., Welsh, M., Kong, Y., Zerhusen, B., Malcolm, R., Varrone, Z., Collis, A., Minto, M., Burgess, S., McDaniel, L., Stimpson, E., Spriggs, F., Williams, J., Neurath, K., Ioime, N., Agee, M., Voss, E., Furtak, K., Renzulli, R., Aanensen, N., Carrolla, S., Bickelhaupt, E., Lazovatsky, Y., DaSilva, A., Zhong, J., Stanyon, C.A., Finley, R.L., Jr., White, K.P., Braverman, M., Jarvie, T., Gold, S., Leach, M., Knight, J., Shimkets, R.A., McKenna, M.P., Chant, J., Rothberg, J.M., 2003. A protein interaction map of Drosophila melanogaster. Science 302, 1727-1736.
Glatter, T., Schittenhelm, R.B., Rinner, O., Roguska, K., Wepf, A., Junger, M.A., Kohler, K., Jevtov, I., Choi, H., Schmidt, A., Nesvizhskii, A.I., Stocker, H., Hafen, E., Aebersold, R., Gstaiger, M., 2011. Modularity and hormone sensitivity of the Drosophila melanogaster insulin receptor/target of rapamycin interaction proteome. Molecular systems biology 7, 547.
Harris, R.M., Pfeiffer, B.D., Rubin, G.M., Truman, J.W., 2015. Neuron hemilineages provide the functional ground plan for the Drosophila ventral nervous system. eLife 4.
Hartman, N.W., Lin, T.V., Zhang, L., Paquelet, G.E., Feliciano, D.M., Bordey, A., 2013. mTORC1 targets the translational repressor 4E-BP2, but not S6 kinase 1/2, to regulate neural stem cell self-renewal in vivo. Cell reports 5, 433-444.
Isshiki, T., Pearson, B., Holbrook, S., Doe, C.Q., 2001. Drosophila neuroblasts sequentially express transcription factors which specify the temporal identity of their neuronal progeny. Cell 106, 511-521.
Kambadur, R., Koizumi, K., Stivers, C., Nagle, J., Poole, S.J., Odenwald, W.F., 1998. Regulation of POU genes by castor and hunchback establishes layered compartments in the Drosophila CNS. Genes Dev 12, 246-260.
Lee, T., Luo, L., 1999. Mosaic analysis with a repressible cell marker for studies of gene function in neuronal morphogenesis. Neuron 22, 451-461.

Li, N., Liu, Q., Xiong, Y., Yu, J., 2019. Headcase and Unkempt Regulate Tissue Growth and Cell Cycle Progression in Response to Nutrient Restriction. Cell reports 26, 733-747.e733.
Li, X., Erclik, T., Bertet, C., Chen, Z., Voutev, R., Venkatesh, S., Morante, J., Celik, A., Desplan, C., 2013. Temporal patterning of Drosophila medulla neuroblasts controls neural fates. Nature 498, 456-462.
Maurange, C., Cheng, L., Gould, A.P., 2008. Temporal transcription factors and their targets schedule the end of neural proliferation in Drosophila. Cell 133, 891-902.
McNeill, H., Craig, G.M., Bateman, J.M., 2008. Regulation of neurogenesis and epidermal growth factor receptor signaling by the insulin receptor/target of rapamycin pathway in Drosophila. Genetics 179, 843-853.
Mohler, J., Weiss, N., Murli, S., Mohammadi, S., Vani, K., Vasilakis, G., Song, C.H., Epstein, A., Kuang, T., English, J., et al., 1992. The embryonically active gene, unkempt, of Drosophila encodes a Cys3His finger protein. Genetics 131, 377-388.
Murn, J., Teplova, M., Zarnack, K., Shi, Y., Patel, D.J., 2016. Recognition of distinct RNA motifs by the clustered CCCH zinc fingers of neuronal protein Unkempt. Nature structural & molecular biology 23, 16-23.
Murn, J., Zarnack, K., Yang, Y.J., Durak, O., Murphy, E.A., Cheloufi, S., Gonzalez, D.M., Teplova, M., Curk, T., Zuber, J., Patel, D.J., Ule, J., Luscombe, N.M., Tsai, L.H., Walsh, C.A., Shi, Y., 2015. Control of a neuronal morphology program by an RNA-binding zinc finger protein, Unkempt. Genes Dev 29, 501-512.
Nagarkar-Jaiswal, S., Lee, P.T., Campbell, M.E., Chen, K., Anguiano-Zarate, S., Gutierrez, M.C., Busby, T., Lin, W.W., He, Y., Schulze, K.L., Booth, B.W., Evans-Holm, M., Venken, K.J., Levis, R.W., Spradling, A.C., Hoskins, R.A., Bellen, H.J., 2015. A library of MiMICs allows tagging of genes and reversible, spatial and temporal knockdown of proteins in Drosophila. eLife 4.
Narbonne-Reveau, K., Lanet, E., Dillard, C., Foppolo, S., Chen, C.H., Parrinello, H., Rialle, S., Sokol, N.S., Maurange, C., 2016. Neural stem cell-encoded temporal patterning delineates an early window of malignant susceptibility in Drosophila. eLife 5.
Paridaen, J.T., Huttner, W.B., 2014. Neurogenesis during development of the vertebrate central nervous system. EMBO reports 15, 351-364.
Potter, C.J., Huang, H., Xu, T., 2001. Drosophila Tsc1 functions with Tsc2 to antagonize insulin signaling in regulating cell growth, cell proliferation, and organ size. Cell 105, 357-368.

Ren, Q., Yang, C.P., Liu, Z., Sugino, K., Mok, K., He, Y., Ito, M., Nern, A., Otsuna, H., Lee, T., 2017. Stem Cell-Intrinsic, Seven-up-Triggered Temporal Factor Gradients Diversify Intermediate Neural Progenitors. Curr Biol 27, 1303-1313.
Shaw, R.E., Kottler, B., Ludlow, Z.N., Buhl, E., Kim, D., Morais da Silva, S., Miedzik, A., Coum, A., Hodge, J.J., Hirth, F., Sousa-Nunes, R., 2018. In vivo expansion of functionally integrated GABAergic interneurons by targeted increase in neural progenitors. Embo j 37.
Sousa-Nunes, R., Cheng, L.Y., Gould, A.P., 2010. Regulating neural proliferation in the Drosophila CNS. Curr Opin Neurobiol 20, 50-57.
Sousa-Nunes, R., Yee, L.L., Gould, A.P., 2011. Fat cells reactivate quiescent neuroblasts via TOR and glial insulin relays in Drosophila. Nature 471, 508-512.
Steneberg, P., Samakovlis, C., 2001. A novel stop codon readthrough mechanism produces functional Headcase protein in Drosophila trachea. EMBO reports 2, 593-597.
Stocker, H., Radimerski, T., Schindelholz, B., Wittwer, F., Belawat, P., Daram, P., Breuer, S., Thomas, G., Hafen, E., 2003. Rheb is an essential regulator of S6K in controlling cell growth in Drosophila. Nat Cell Biol 5, 559-565.
Suzuki, T., Kaido, M., Takayama, R., Sato, M., 2013. A temporal mechanism that produces neuronal diversity in the Drosophila visual center. Dev Biol 380, 12-24.
Syed, M.H., Mark, B., Doe, C.Q., 2017. Steroid hormone induction of temporal gene expression in Drosophila brain neuroblasts generates neuronal and glial diversity. eLife 6.
Taverna, E., Gotz, M., Huttner, W.B., 2014. The cell biology of neurogenesis: toward an understanding of the development and evolution of the neocortex. Annu Rev Cell Dev Biol 30, 465-502.
Tee, A.R., Sampson, J.R., Pal, D.K., Bateman, J.M., 2016. The role of mTOR signalling in neurogenesis, insights from tuberous sclerosis complex. Semin Cell Dev Biol 52, 12-20.
Truman, J.W., Bate, M., 1988. Spatial and temporal patterns of neurogenesis in the central nervous system of Drosophila melanogaster. Dev Biol 125, 145-157.
Veraksa, A., Bauer, A., Artavanis-Tsakonas, S., 2005. Analyzing protein complexes in Drosophila with tandem affinity purification-mass spectrometry. Dev Dyn 232, 827-834.
Viktorin, G., Riebli, N., Reichert, H., 2013. A multipotent transit-amplifying neuroblast lineage in the central brain gives rise to optic lobe glial cells in Drosophila. Dev Biol 379, 182-194.
Weaver, T.A., White, R.A., 1995. headcase, an imaginal specific gene required for adult morphogenesis in Drosophila melanogaster. Development 121, 4149-4160.

Weng, M., Lee, C.Y., 2011. Keeping neural progenitor cells on a short leash during Drosophila neurogenesis. Curr Opin Neurobiol 21, 36-42.
Zhu, S., Lin, S., Kao, C.F., Awasaki, T., Chiang, A.S., Lee, T., 2006. Gradients of the Drosophila Chinmo BTB-zinc finger protein govern neuronal temporal identity. Cell 127, 409-422.

Figures

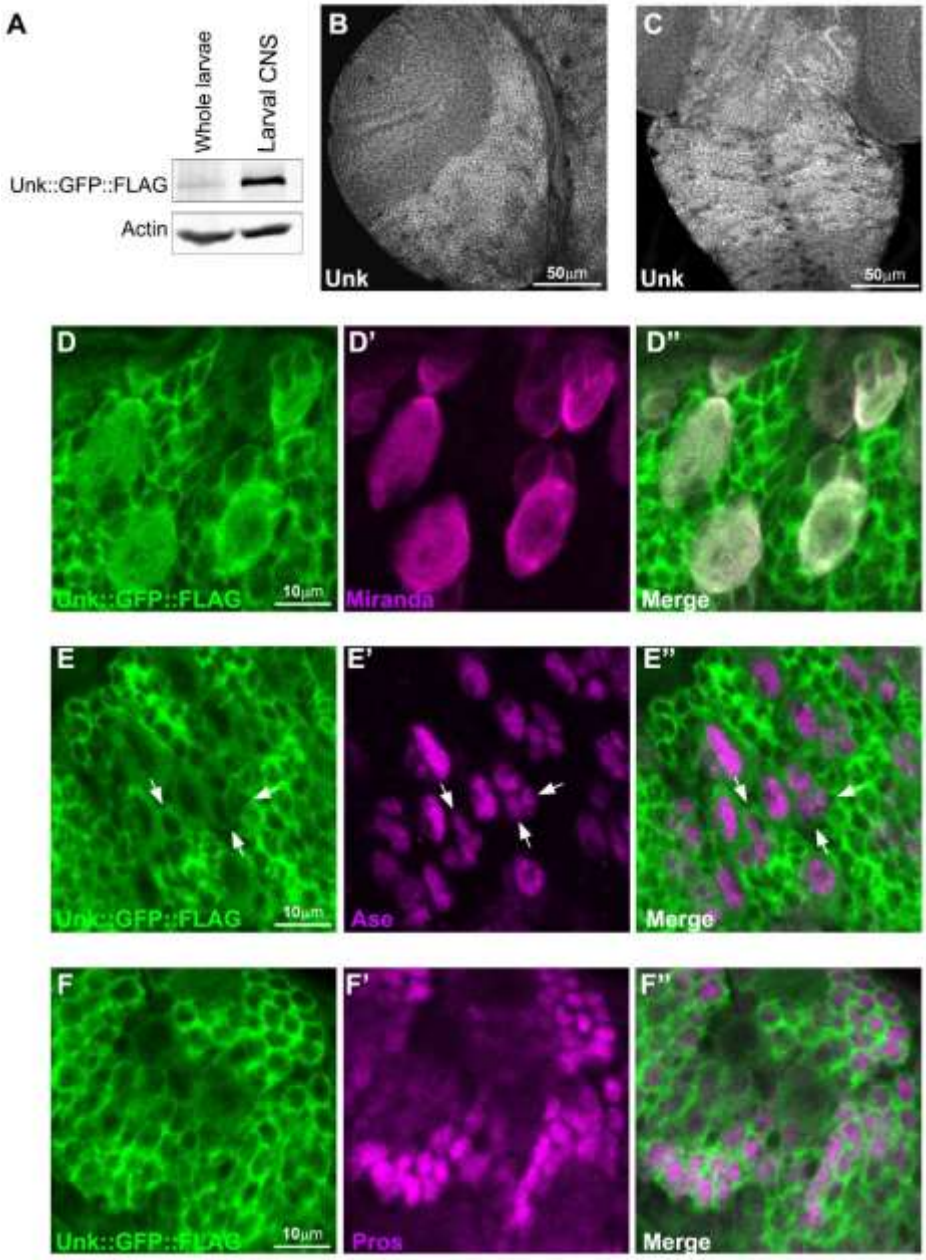

Figure. 1. Unk expression is enriched in the central brain and thoracic VNC. (A) Western blot analysis using an anti-GFP antibody of late third instar whole larvae and larval CNS tissue expressing Unk::GFP::FLAG. Actin expression is shown as a loading control. (B, C) Wild-type larval brain hemisphere (B) and VNC (C) immunostained for Unk. (D-E'') Expression of Unk::GFP::FLAG (green in D, D'', E, E'', F, F'') in the late third instar larval VNC together with Miranda (magenta in D', D'') marking neuroblasts, Asense marking neuroblasts and GMCs (Ase, magenta in E', E''), and Prospero (Pros, magenta in F', F'') marking neurons in this image, although Prospero expression is not specific to neurons. GMCs are indicated by arrows in (E-E'').

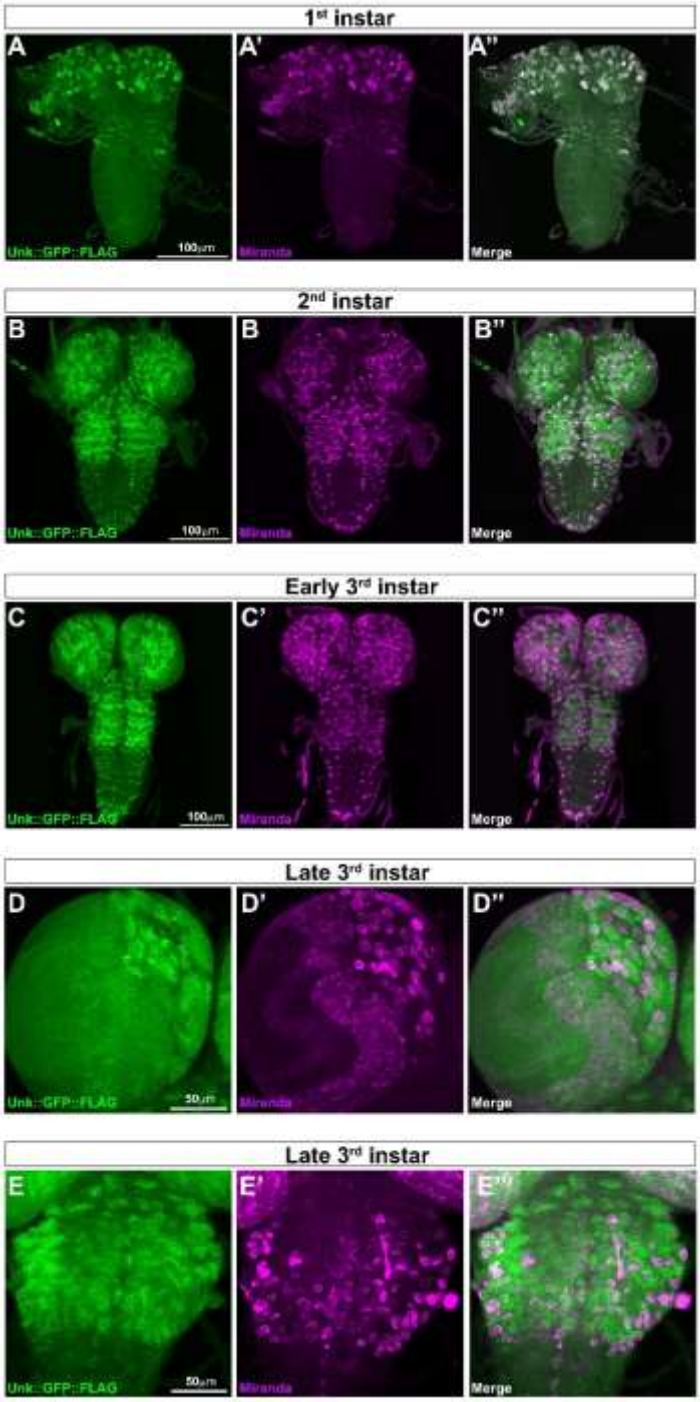

Figure 2. Unk is expressed throughout the neuronal lineage during postembryonic development. (A-C'') Unk::GFP::FLAG expression (green) in first (A-A''), second (B-B'') and early third (C-C'') instar larvae. (D-E'') Unk::GFP::FLAG expression (green) in the late third instar central brain and optic lobe (D-D'') and VNC (E-E''). Neuroblasts are marked by Miranda expression (magenta).

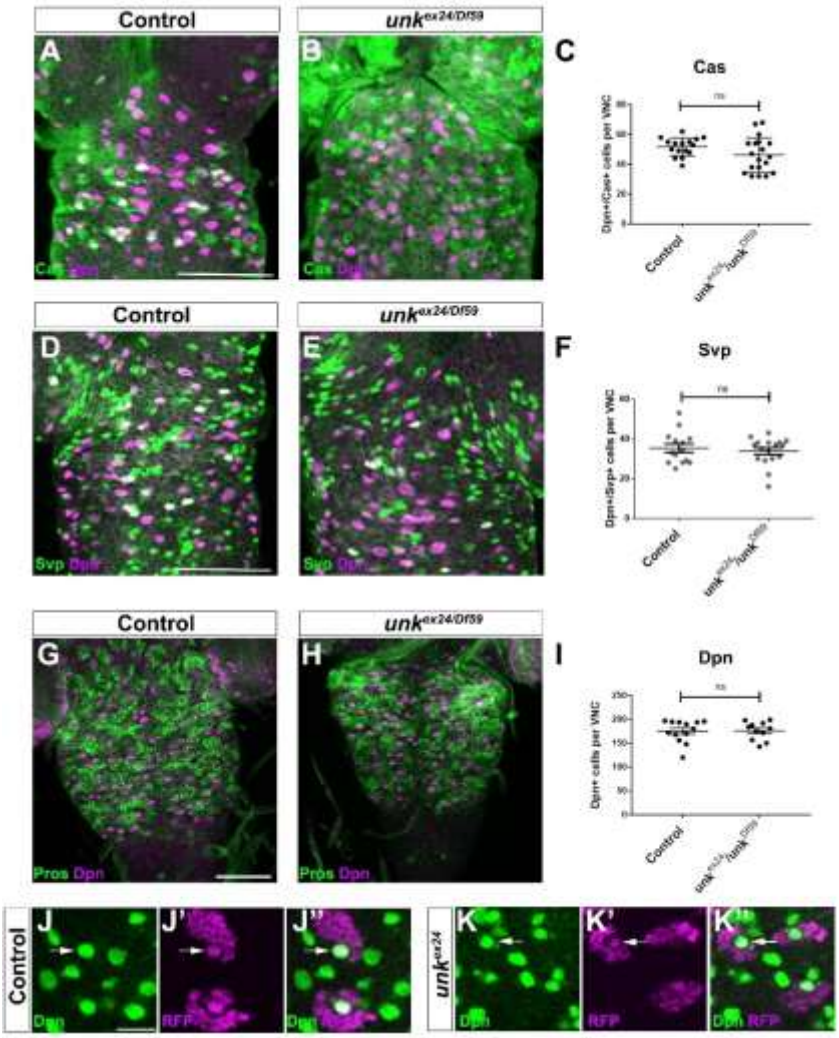

Figure. 3. Loss of Unk does not affect the temporal series or neuroblast numbers. (A, B) Expression of Cas (green) and Dpn (magenta) in control (A) and unk^{ex24}/unk^{Df59} (B) thoracic VNCs at 48 hours ALH. Scale bar 50 μm. (C) Quantification of Cas/Dpn expressing neuroblasts in the thoracic VNC at 48 hours ALH. Control n=16; unk^{ex24}/unk^{Df59} n=19. (D, E) Expression of Svp (green) and Dpn (magenta) in control (D) and unk^{ex24}/unk^{Df59} (E) thoracic VNCs at 48 hours ALH. Scale bar 50 μm. (F) Quantification of Svp/Dpn expressing neuroblasts in the CNS at 48 hours ALH. Control n=14; unk^{ex24}/unk^{Df59} n=17. (G, H) Dpn expressing neuroblasts (magenta) in control (G) and unk^{ex24}/ unk^{Df59} (H) thoracic VNC at 96 hours ALH, co-stained for Prospero (Pros, green). Scale bar 50 μm. (I) Quantification of Dpn expressing neuroblasts in the thoracic VNC at 96 hours ALH. Control n=14; unk^{ex24}/unk^{Df59} n=12. (J-K'') Expression of Dpn (green) in control (J-J'') and unk^{ex24} (K-K'') thoracic MARCM clones (marked by RFP expression, magenta) at 96 hours ALH. Arrows indicate neuroblasts. Scale bar 20 μm. Data are represented as mean +/- SEM, ns: not significant. Student's t test was used for statistical analyses.

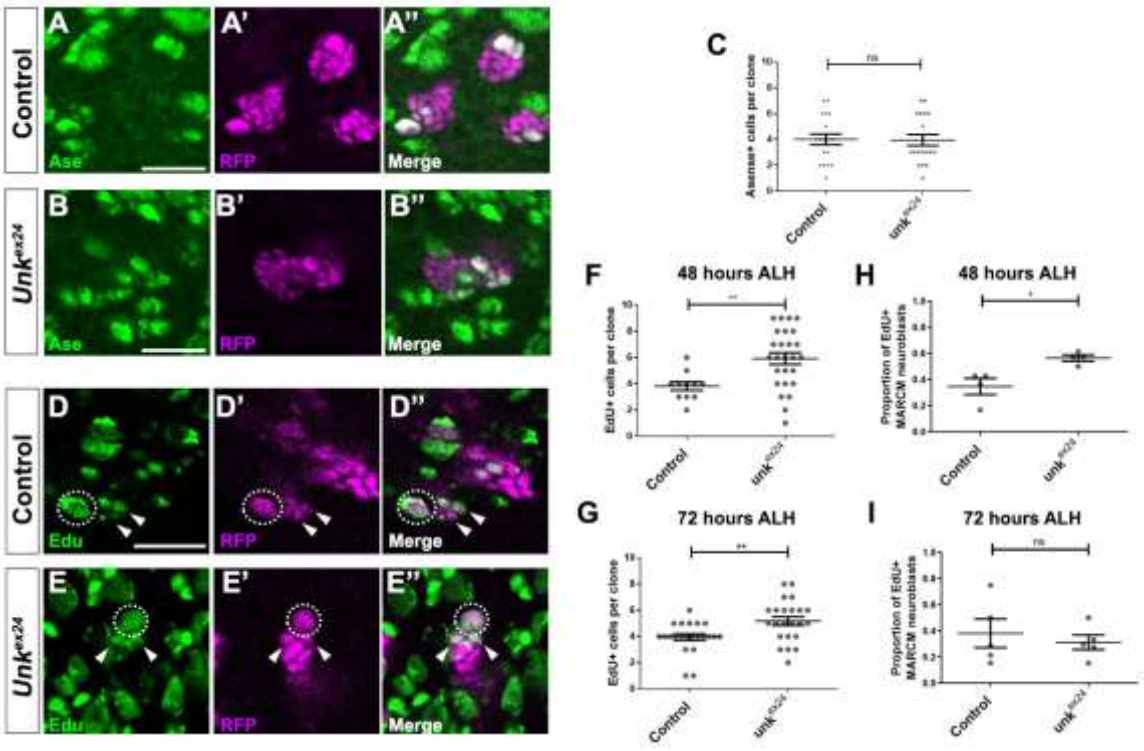

Figure. 4. Unk negatively regulates S-phase in neuroblasts and GMCs. (A-B'') Asense (Ase) expression (green) in control (A-A'') and *unk*^{ex24} (B-B'') thoracic MARCM clones (marked by RFP expression, magenta) at 96 hours ALH. (C) Quantification of Asense expressing cells in thoracic VNC MARCM clones. Control n=19; *unk*^{ex24} n=19. (D-E'') *Ex vivo* EdU labelling (green) in control (D-D'') and *unk*^{ex24} (E-E'') thoracic MARCM clones (marked by RFP expression, magenta) at 72 hours ALH. (F, G) Quantification of EdU labelled cells per thoracic VNC MARCM clone at 48 hours (F) and 72 hours ALH (G). For 48 hours ALH control n=11; *unk*^{ex24} n=25. For 72 hours ALH control n=22; *unk*^{ex24} n=23. (H, I) Quantification of the proportion of MARCM clone neuroblasts labelled with EdU at 48 hours (H) and 72 hours ALH (I). For 48 hours ALH control n=4 VNCs; *unk*^{ex24} n=4 VNCs. For 72 hours ALH control n=5 VNCs; *unk*^{ex24} n=5 VNCs. Data are represented as mean +/- SEM, ns: not significant, ** $p<0.01$. Scale bar 20 μm. Student's t test was used for statistical analyses.

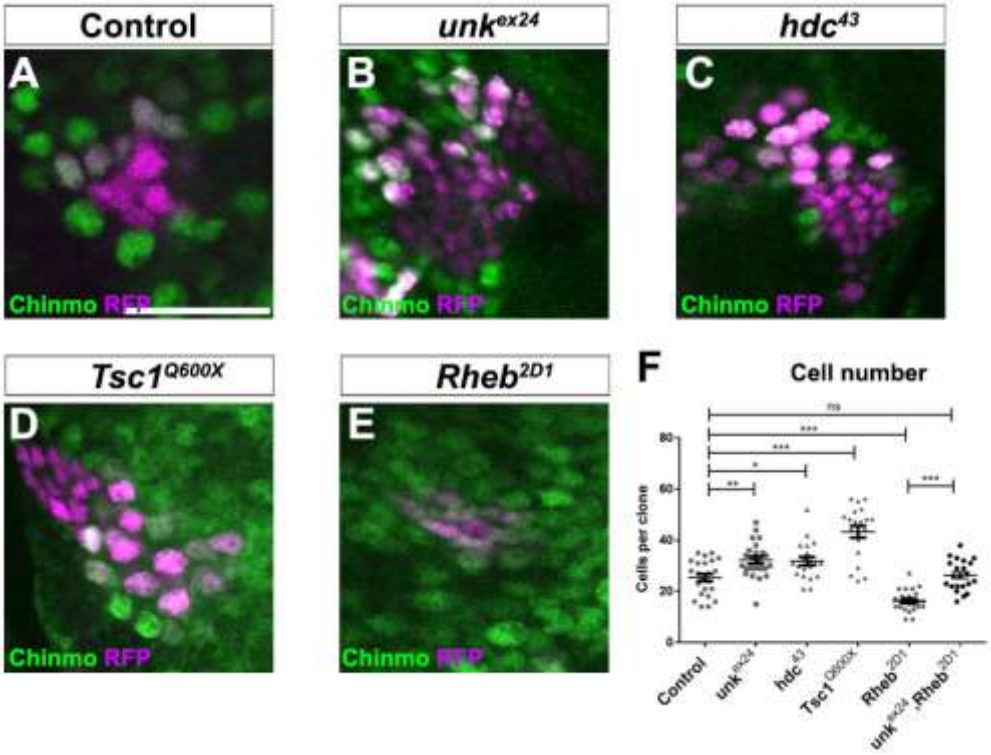

Figure. 5. Unk and Hdc negatively regulate neurogenesis. (A-E) Control (A), *unk*^{ex24} (B), *hdc*^{43} (C), *Tsc1*^{Q600X} (D) and *Rheb*^{2D1} (E) thoracic VNC MARCM clones (marked by RFP expression, magenta) at 96 hours ALH. Chinmo expression (green) marks early born neurons. (F) Quantification of number of cells per thoracic VNC MARCM clone. Control n=22; *unk*^{ex24} n=24; *hdc*^{43} n=20; *Tsc1*^{Q600X} n=20; *Rheb*^{2D1} n=24; *unk*^{ex24}, *Rheb*^{2D1} n=22. Data are represented as mean +/- SEM, ns: not significant, * p<0.05, ** p<0.01, *** p<0.001. Scale bar 50 μm. One-way ANOVA was used for statistical analysis.

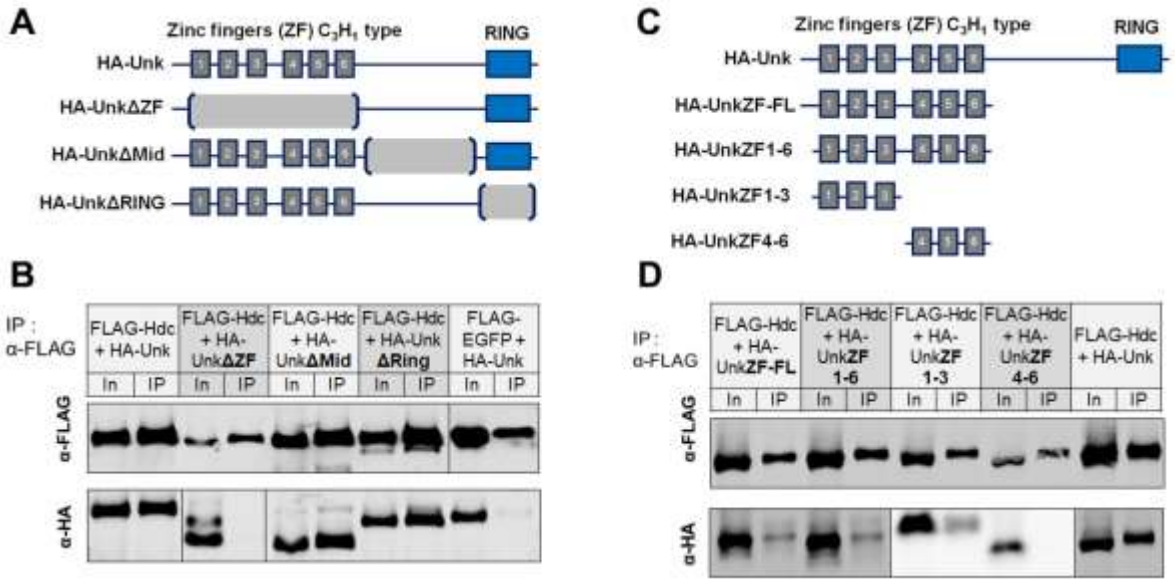

Figure. 6. Unk physically interacts with Hdc via its zinc finger domain. (A) Schematic of HA-tagged Unk deletion mutants. Grey boxes indicate deleted regions. (B) Western blot analysis after using an anti-FLAG antibody to immunoprecipitate FLAG-Hdc from S2 cells co-transfected with HA-tagged full length Unk or Unk mutants. FLAG-EGFP was used as a negative control. (C) Schematic of HA-tagged Unkempt zinc finger constructs. (D) Western blot analysis after using an anti-FLAG antibody to immunoprecipitate FLAG-Hdc from S2 cells co-transfected with HA-tagged Unk zinc finger constructs. In: input from S2 cell lysate, IP: after immunoprecipitation.

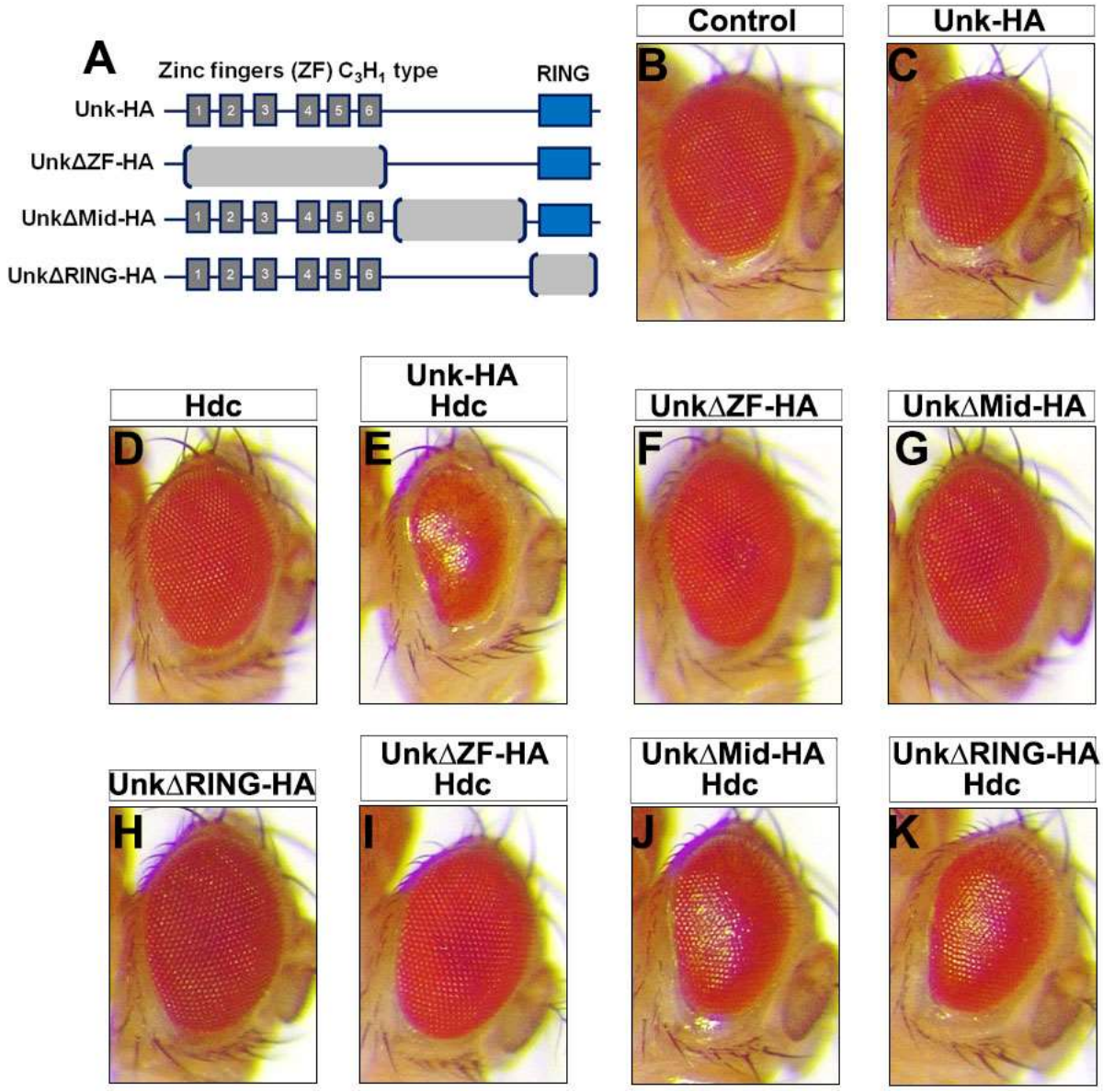

Figure 7. The zinc finger domain is necessary for the overexpression activity of Unk in the eye. (A) Schematic of HA-tagged Unk deletion mutants. Grey boxes indicate deleted regions. (B-E) Control (*GMR-GAL4*/+), or *GMR-GAL4* driven overexpression of Unk-HA alone (C), Hdc alone (D), or Unk-HA and Hdc simultaneously (E). (F-H) Overexpression of Unk mutants lacking the zinc finger domain (F, UnkΔZF-HA), the middle region (G, UnkΔMid-HA), or the RING domain (H, UnkΔRING-HA) alone using *GMR-GAL4*. (I-K) Overexpression of UnkΔZF-HA (I), UnkΔMid-HA (J), or UnkΔRING-HA (K) together with Hdc using *GMR-GAL4*.

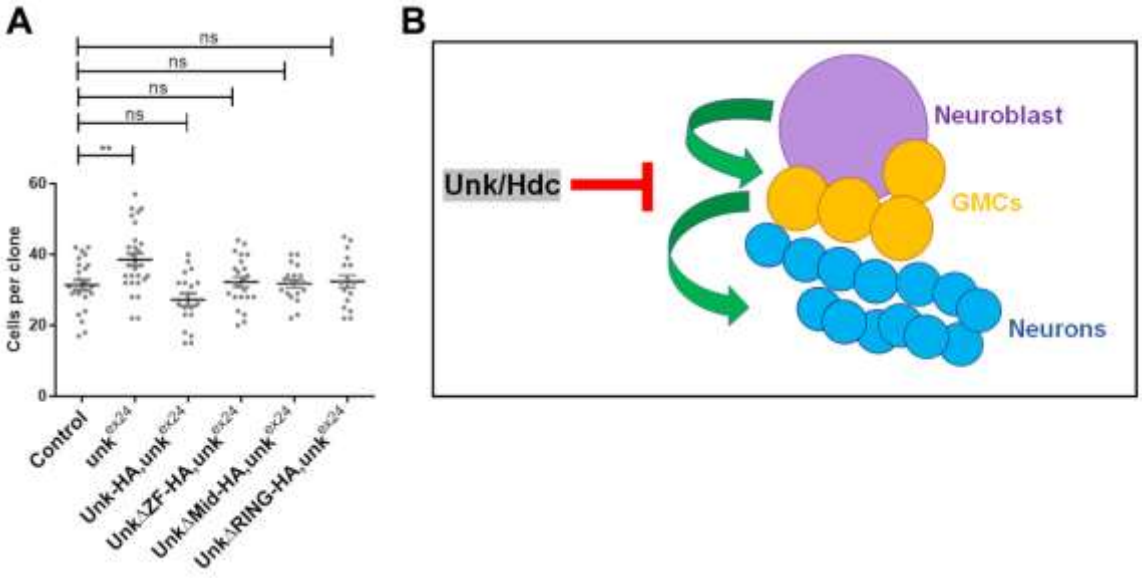

Figure. 8. The zinc finger domain of Unk is not necessary for regulation of neurogenesis. (A) Quantification of number of cells per thoracic MARCM clone at 96 hours ALH in control, unk^{ex24} or unk^{ex24} clones expressing full length or *unk* deletion mutants. Data are represented as mean +/- SEM, ns: not significant, ** $p<0.01$. Control n=25; unk^{ex24} n=45; Unk-HA, unk^{ex24} n=19; UnkΔZF-HA, unk^{ex24} n=23; UnkΔMid-HA, unk^{ex24} n=19 ; UnkΔRING-HA, unk^{ex24} n=17. (B) A model illustrating the role of Unk and Hdc in neurogenesis in the *Drosophila* CNS. One-way ANOVA was used for statistical analysis.

Supplemental figures

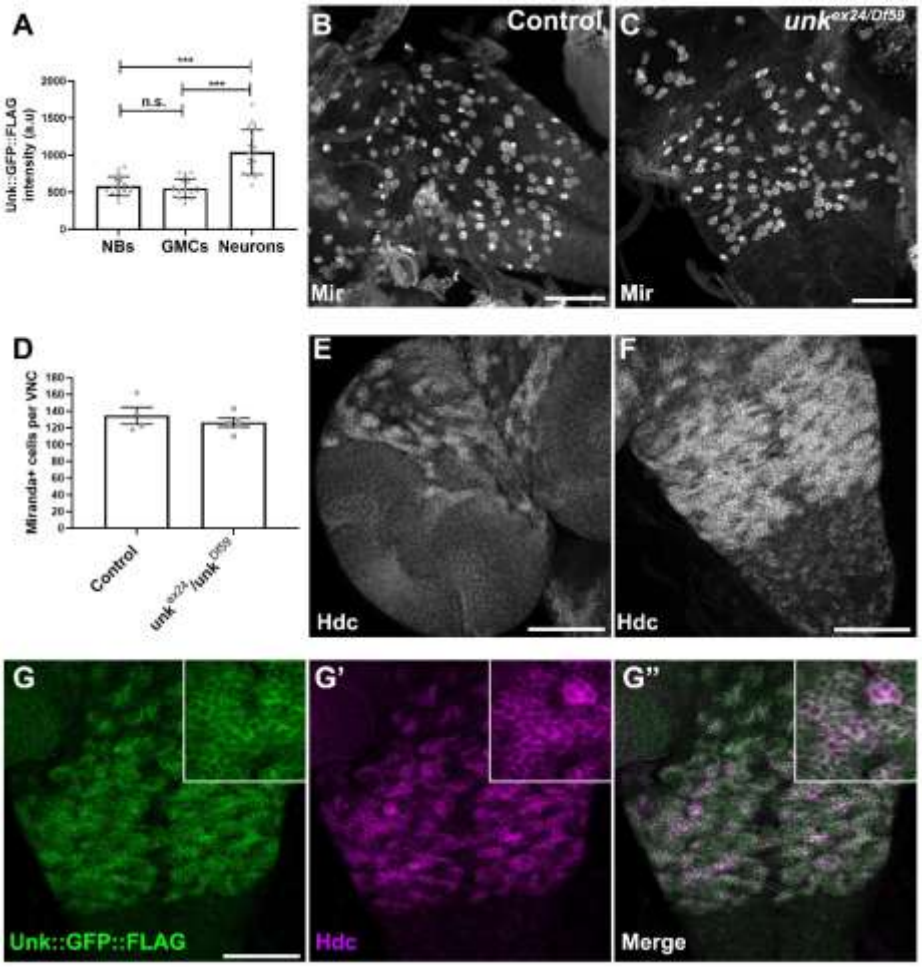

Figure S1. Hdc colocalises with Unk in the CNS. (A) Quantification of Unk::GFP::FLAG expression in late third instar neuroblasts (NBs, n=20), GMCs (n=20) and neurons (n=20). One-way ANOVA was used for statistical analysis. (B, C) Miranda expressing neuroblasts in control (B) and unk^{ex24}/unk^{Df59} (C) VNC at 10 hours APF. (D) Quantification of VNC neuroblasts at 10 hours APF. Control n=4 VNCs; unk^{ex24}/unk^{Df59} n=5 VNCs. Student's t test was used for statistical analysis. (E, F) Wild-type larval brain hemisphere (E) and VNC (F) immunostained for Hdc. (G-G'') Unk::GFP::FLAG (green) expressing larval VNC immunostained for Hdc (magenta). Insets show magnified regions. Scale bar is 50 μm. Data are represented as mean +/- SEM, ns: not significant, *** $p<0.001$.

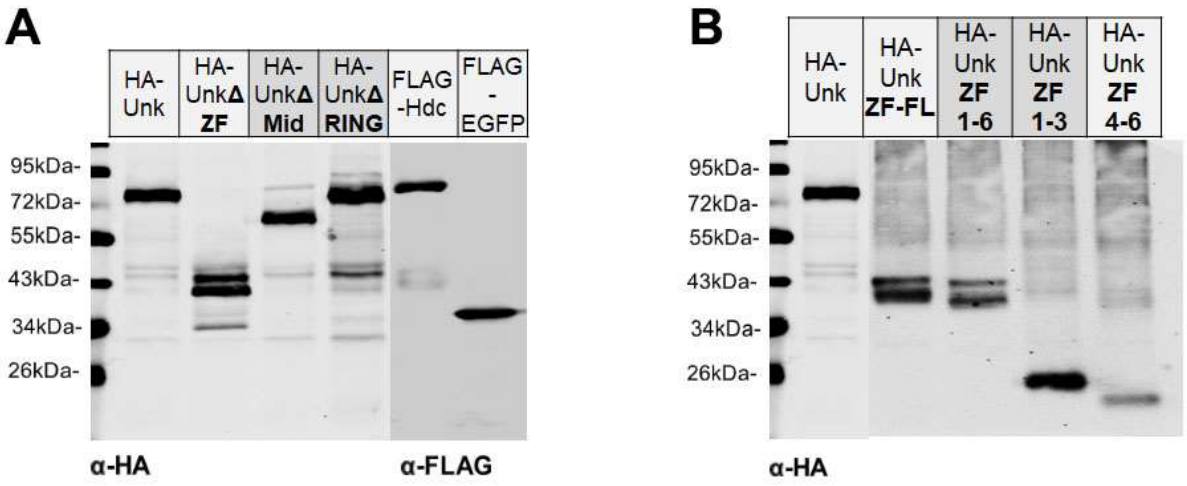

Figure S2. Western blot analysis of Unk mutant expression in S2 cells. (A) HA-tagged full length Unk or Unk deletion mutants expressed in S2 cells. Expression of FLAG-Hdc and FLAG-EGFP are also shown. (B) HA-tagged full length Unk and Unk zinc finger constructs expressed in S2 cells.

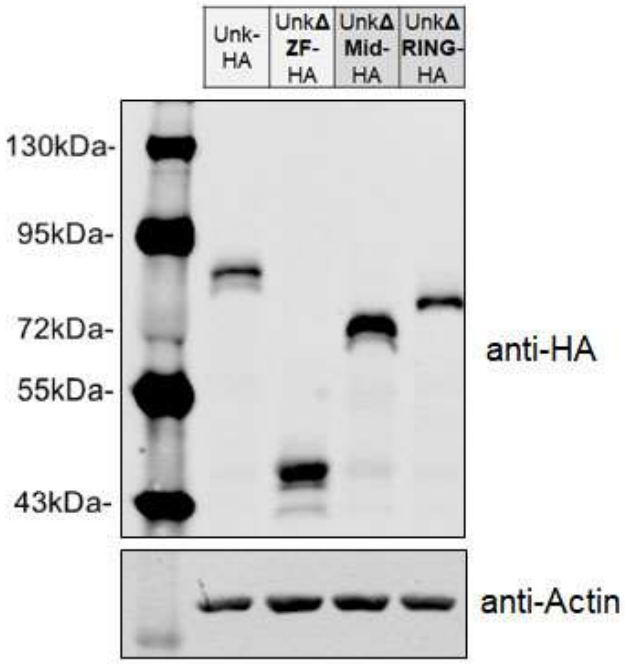

Figure S3. Western blot analysis of Unk deletion mutant expression in vivo. Western blot analysis of CNS tissue from late third instar larvae using *Hs-GAL4* to express HA-tagged full length Unk or Unk deletion mutants. Actin was used as a loading control.

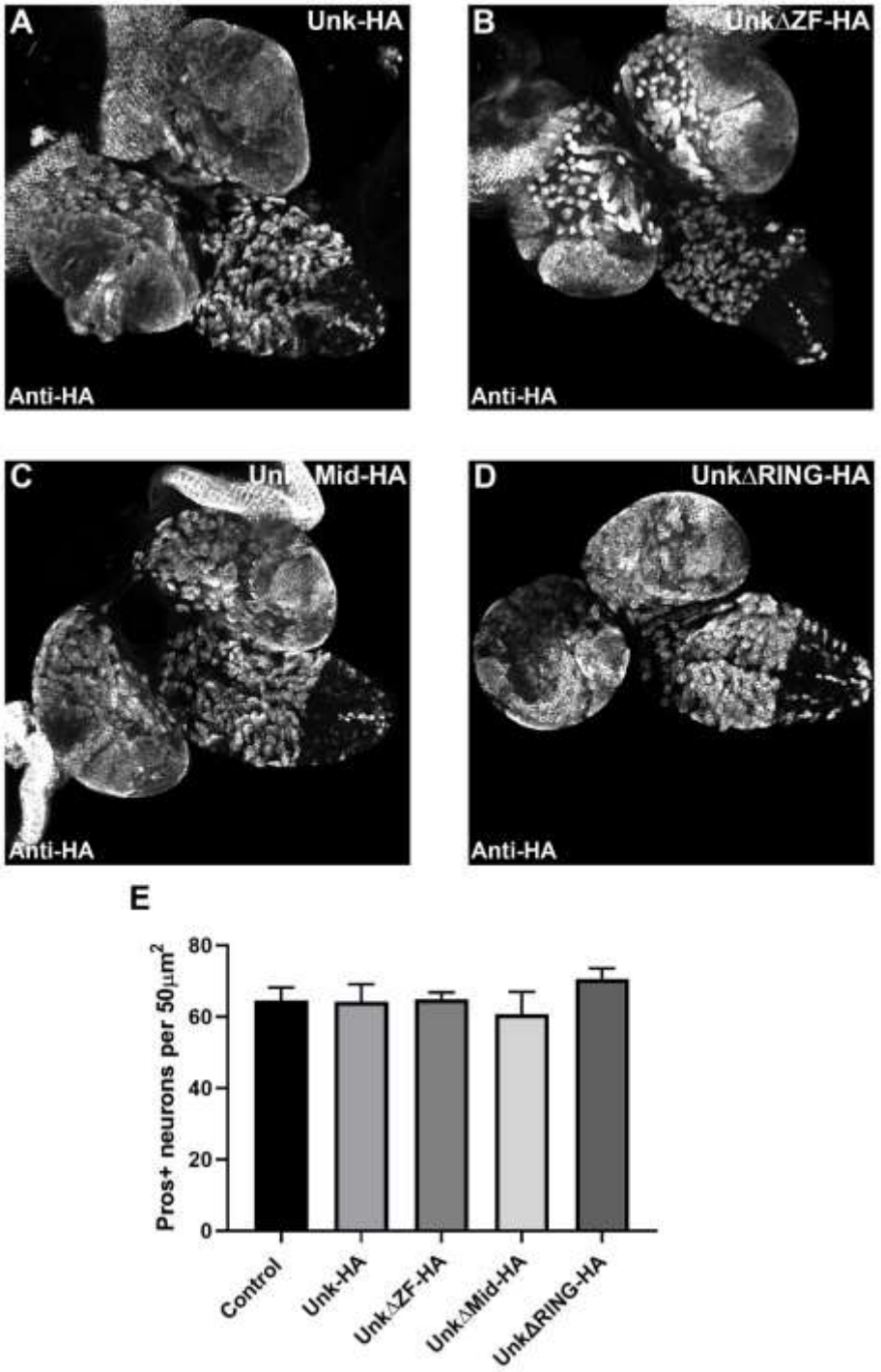

Figure S4. Overexpression of Unk transgenes in the CNS. (A-D) *Elav-Gal4* driven expression of Unk-HA (A), UnkΔZF-HA (B), UnkΔMid-HA (C) and UnkΔRING-HA (D) in the late third instar CNS stained with anti-HA. (E) Quantification of the number of Prospero expressing neurons in the VNC. Control n=5; Unk-HA n=3; UnkΔZF-HA n=4; UnkΔMid-HA n=4; UnkΔRING-HA n=3. Data are represented as mean +/- SEM. One-way ANOVA was used for statistical analysis.

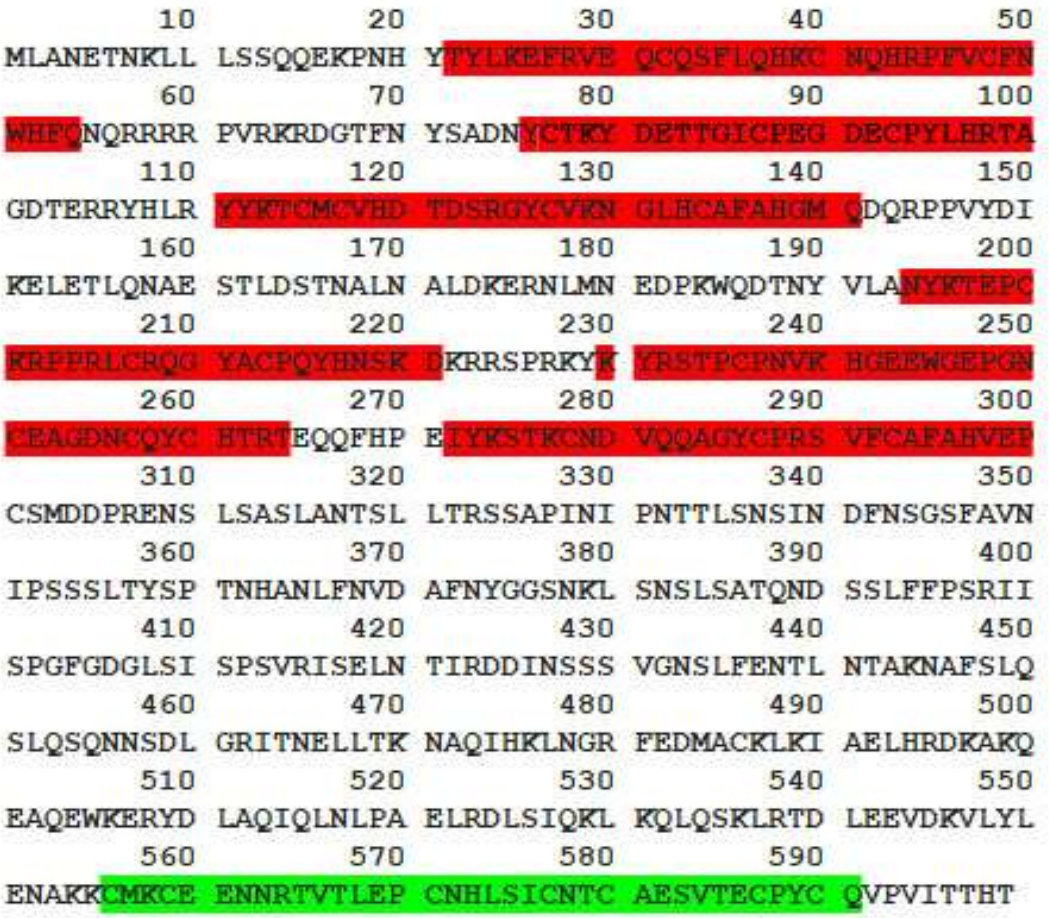

Figure S5. The primary sequence of Drosophila Unk. Zinc finger domains are highlighted in red, the RING domain is highlighted in green.

Supplemental Tables

Table S1. Experimental genotypes

Figure	Label in figure	Genotype
Figure 1	Unk	*w^{1118}*
	Unk::GFP::FLAG	*Mi{PT-GFSTF.2}unk$^{MI09783\text{-}GFSTF.2}$*
Figure 2	Unk::GFP::FLAG	*Mi{PT-GFSTF.21unk$^{MI09783\text{-}GFSTF.2}$*
Figure 3	Control	*w^{1118}*
	unk$^{ex24/Df59}$	*Unk$^{ex24/Df59}$*
	Control	*elav-GAL4^{C155}, UAS-Redstinger, hsFLP^{122}; FRT82B, tub-GAL80/ FRT82B*
	unk^{ex24}	*elav-GAL4^{C155}, UAS-Redstinger, hsFLP^{122}; FRT82B, tub-GAL80/ FRT82B, unk^{ex24}*
Figure 4	Control	*elav-GAL4^{C155}, UAS-Redstinger, hsFLP^{122}; FRT82B, tub-GAL80/ FRT82B*
	unk^{ex24}	*elav-GAL4^{C155}, UAS-Redstinger, hsFLP^{122}; FRT82B, tub-GAL80/ FRT82B, unk^{ex24}*
Figure 5	Control	*elav-GAL4^{C155}, UAS-Redstinger, hsFLP^{122}; FRT82B, tub-GAL80/ FRT82B*
	unk^{ex24}	*elav-GAL4^{C155}, UAS-Redstinger, hsFLP^{122}; FRT82B, tub-GAL80/ FRT82B, unk^{ex24}*
	hdc^{43}	*elav-GAL4^{C155}, UAS-Redstinger, hsFLP^{122}; FRT82B, tub-GAL80/ FRT82B, hdc^{43}*
	Tsc1^{Q600X}	*elav-GAL4^{C155}, UAS-Redstinger, hsFLP^{122}; FRT82B, tub-GAL80/ FRT82B, Tsc1^{Q600X}*
	Rheb^{2D1}	*elav-GAL4^{C155}, UAS-Redstinger, hsFLP^{122}; FRT82B, tub-GAL80/ FRT82B, Rheb^{2D1}*
	unk^{ex24}, Rheb^{2D1}	*elav-GAL4^{C155}, UAS-Redstinger, hsFLP^{122}; FRT82B, tub-GAL80/ FRT82B, unk^{ex24}, Rheb^{2D1}*
Figure 7	Control	*GMR-Gal4/+*
	Unk-HA	*GMR-Gal4/+; UAS-Unk-HA*
	Hdc	*GMR-Gal4/+; UAS-Hdc*
	Unk-HA Hdc	*GMR-Gal4/+; UAS-Unk-HA, UAS-Hdc*
	UnkΔZF-HA	*GMR-Gal4/+; UAS-UnkΔZF-HA*
	UnkΔMid-HA	*GMR-Gal4/+; UAS-UnkΔMid-HA*
	UnkΔRING-HA	*GMR-Gal4/+; UAS-UnkΔRING-HA*
	UnkΔZF-HA Hdc	*GMR-Gal4/+; UAS-UnkΔZF-HA, UAS-Hdc*
	UnkΔMid-HA Hdc	*GMR-Gal4/+; UAS-UnkΔMid-HA, UAS-Hdc*
	UnkΔRING-HA Hdc	*GMR-Gal4/+; UAS-UnkΔRING-HA, UAS-Hdc*
Figure 8	Control	*elav-GAL4^{C155}, UAS-Redstinger, hsFLP^{122}; FRT82B, tub-GAL80/ FRT82B*
	unk^{ex24}	*elav-GAL4^{C155}, UAS-Redstinger, hsFLP^{122}; FRT82B, tub-GAL80/ FRT82B, unk^{ex24}*
	Unk-HA, unk^{ex24}	*elav-GAL4^{C155}, UAS-Redstinger, hsFLP^{122}; FRT82B, tub-GAL80/UAS-Unk-HA, FRT82B, unk^{ex24}*
	UnkΔZF-HA, unk^{ex24}	*elav-GAL4^{C155}, UAS-Redstinger, hsFLP^{122}; FRT82B, tub-GAL80/UAS-UnkΔZF-HA, FRT82B, unk^{ex24}*

	UnkΔMid-HA, unk^{ex24}	*elav-GAL4^{C155}, UAS-Redstinger, hsFLP^{122}; FRT82B, tub-GAL80/UAS-UnkΔMid-HA, FRT82B, unk^{ex24}*
	UnkΔRING-HA, unk^{ex24}	*elav-GAL4^{C155}, UAS-Redstinger, hsFLP^{122}; FRT82B, tub-GAL80/UAS-UnkΔRING-HA, FRT82B, unk^{ex24}*
Figure S1	$unk^{ex24/Df59}$	*Unk$^{ex24/Df59}$*
	Unk::GFP::FLAG	*Mi{PT-GFSTF.2}unk$^{MI09783-GFSTF.2}$*
Figure S4	Control	*elav-GAL4^{C155}/+*
	Unk-HA	*elav-GAL4^{C155}/+; UAS-Unk-HA*
	UnkΔZF-HA	*elav-GAL4^{C155}/+; UAS-UnkΔZF-HA*
	UnkΔMid-HA	*elav-GAL4^{C155}/+; UAS-UnkΔMid-HA*
	UnkΔRING-HA	*elav-GAL4^{C155}/+; UAS-UnkΔRING-HA*

Table S2. Primers used to generate Unk constructs. Homologous overhangs are underlined.

Primer	**Sequence 5'-3'**
Unk deletion constructs	
UnkFWEntr	CACCATGTTGGCAAATGAAACGAACAAGCTGC
UnkRVfusionEntr	GGTGTGGGTGGTTATTACCGGC
UnkΔZF.Fw	CACCATGGTGGAACCTTGCTCAATGGACGAT
UnkΔMid.Fw	GGCCAATACTCTTCAATCTCTGCAGTCGCAAAACAAC
UnkΔMid.Rv	CAGAGATTGAAGAGTATTGGCCAGACTCGCCGACAATGA
UnkΔRING.noStp.Rv	GGCATTTTCTAAATATAATACTTTGTCG
Unk zinc finger constructs	
UnkFWEntr	CACCATGTTGGCAAATGAAACGAACAAGCTGC
UnkZF1-6.Fw	CACCATGCCAAATCACTACACCTACCTGAAG
UnkZF1-6.noStp.Rv	TTTGCCCATGTGGAACCTTGCTCA
UnkZF1-3.Rv	AAAGAGCTGGAGACCCTGCAGAACTAG
UnkZF4-6.Fw	CACCATGCCCAAGTGGCAGGACACCAACTA